# Dynamic Mechanical Study of the Factors Affecting the Two Glass Transition Behavior of Filled Polymers. Similarities and Differences with Random Ionomers

**George Tsagaropoulos and Adi Eisenberg***

*Department of Chemistry, McGill University, 801 Sherbrooke Street West, Montréal, Québec, Canada H3A 2K6*

*Received March 13, 1995; Revised Manuscript Received May 15, 1995*[⊗]

ABSTRACT: The dynamic mechanical measurements on several polymers filled with very fine silica particles revealed that these composites exhibit two tan $\delta$ peaks. One was related to the usual polymer glass transition, while the other, occurring at a higher temperature, was assigned to the glass transition of regions containing chains of reduced mobility. Since many aspects of this behavior were found to be analogous to those of random ionomers, the results support the validity of the EHM model of ionomer morphology. The particle content, the number of monomer units interacting strongly with the surface of the particles, the thermal history of the sample, and the average MW of the polymer were all found to have a significant effect on the area and the maximum of the new tan $\delta$ peak. These effects are discussed in terms of a model which is based on the EHM ionomer model but takes into account the formation of tightly bound and loosely bond polymer chains around the filler particles.

## Introduction

Random ionomers are usually polymers typically containing up to 20 mol % ionic groups, randomly distributed along the polymer chains. Many of these polymers, regardless of the nature of the ionic groups or sometimes even that of the matrix chains, are characterized by similar mechanical properties. For many systems, time–temperature superposition fails above a certain ion content; also, the materials exhibit two glass transitions. The detailed characteristics of the corresponding tan $\delta$ peaks, including the glass transition temperature and the area of the peaks, depend on the specifics of the system under investigation.[1]

Over the past 30 years, several theoretical attempts to explain this complex behavior have appeared. Usually, the models postulate a particular morphology which, in turn, dictates the mechanical properties of the ionomer. It is generally accepted that in ionomers several ionic groups assemble into moieties called multiplets. In the most recent model proposed by Eisenberg, Hird, and Moore (abbreviated EHM model), the multiplets are thought to restrict the mobility of polymer chains around them. Above a certain ion content, characteristic of the particular ionomer, the regions of restricted mobility start to overlap, and when their size exceeds *ca.* 5–10 nm, they exhibit their own glass transition at a temperature which is considerably higher than that of the nonionic polymer.[2] Other models have also been proposed, for example the "core–shell" model of a MacKnight and co-workers,[3a] or the "hard sphere" model of Cooper *et al.*[3b]

Although the EHM model is in agreement with a very wide range of experimental observations, data supporting the existence of restricted mobility regions in random ionomers are still only fragmentary. DSC measurements of the heat capacity change at the glass transition of sulfonated polystyrene ionomers, reported by Risen and co–workers,[4] indicated that at high ion contents, some styrene units adjacent to sulfonated sites were constrained from participating in the glass transition. Dielectric[5] and NMR[6,7] measurements on telechelic and block ionomers, which are considered to be model materials for random ionomers, showed that the mobility of monomer units near the multiplets or ionic cores is reduced. Thus, the experimental evidence supports the notion of the EHM model that mobility restrictions are operative in ionomeric systems.

An important question to be answered is whether the restricted mobility regions in polymers, regardless of the mechanism of their generation, can give rise to increases in $T_g$ as large as those suggested by the EHM model and observed experimentally. To address the question most generally, a nonionic polymer system has to be examined, which contains regions of different chain mobilities. The systems selected in our work are several polymers filled with very fine silica particles. These composite materials are known to contain regions of restricted mobility due to the presence of polymer–filler interactions. It is our intention to show that when the particle size is very small, and the interactions are strong enough, then, as predicted by Kim *et al.*,[8] these materials exhibit two glass transitions. If this is indeed the case, then a major point of the EHM model, namely that the regions of restricted mobility can exhibit their own glass transition, can be considered proven.

The morphologies and the properties of filled polymers have been studied extensively in the past. Nearly every technologically significant aspect of the properties and behavior of rubbers reinforced with carbon black particles has been investigated owing to the importance of these materials. Several monographs and review articles over the years have summarized the vast literature on this subject.[9] It is considerably beyond the scope of this introduction to review all the aspects of filled polymer behavior. Instead, only those aspects will be discussed having a direct bearing on the present study in that they consider polymer dynamics near surfaces which could be related to new relaxation phenomena in these materials.

The effect of filler particles on the mobility of polymer chains has been studied in the past by several techniques, including dilatometry,[10] DSC,[11] and very recently, neutron scattering.[12] Important insight was gained, though, by NMR relaxation time measurements

[⊗] Abstract published in *Advance ACS Abstracts,* August 1, 1995.

0024-9297/95/2228-6067$09.00/0 

on filled rubbers, carried out by several research groups in the last two decades.[13-16] These experiments revealed the existence of rubber regions characterized by different mobilities. In the immediate vicinity of the particle surface, there was a rubber layer with a very low spin–spin relaxation time ($T_2$), which did not change significantly when the sample was heated through the rubber glass transition. This layer was almost immobile. The material beyond this layer exhibited the usual glass transition, but the $T_2$ value measured at temperatures above the $T_g$ was 1 order of magnitude lower than the $T_2$ of the unfilled rubber. This difference reflects the existence of a restricted mobility layer. McBrierty *et al.*[14] calculated the thickness of the two layers using an equation derived by Pliskin and Tokita.[17] Generally, the thickness of the immobile layer varied between 5 and 20 Å, while the restricted mobility layer was between 25 and 90 Å thick, depending on the size and the volume fraction of carbon black particles.

These experiments, although useful in revealing that indeed filler particles restrict chain mobility, do not answer the question of whether or not mobility restrictions can generally cause a second glass transition. It is thus essential to examine how these existing restrictions affect the dynamic mechanical properties of filled polymers. Ecker[18] measured the dynamic mechanical properties of lightly cross-linked SBR, filled with carbon black particles as a function of temperature. Several changes in the loss and storage moduli were observed in the high-temperature region with increasing carbon black content, amounting to the appearance of a second tan $\delta$ peak in filled samples. St. Pierre and co-workers[19] measured the tan $\delta$ curves using a torsion pendulum technique, for several polymers filled with fine silica particles. Two tan $\delta$ peaks appeared in the case of PDMS. The lower temperature peak was assigned to the usual glass transition of PDMS, while the other was attributed to the glass transition of chains adsorbed on the particle surface. For the other polymers (polystyrene, poly(ethylene glycol), and ethylene–propylene rubber) examined in that study, only a single tan $\delta$ peak was observed. A shift in $T_g$ was noticed, and it was related to the adsorption energy of model small molecules on the silica particles. Recently, Landry *et al.*[20] compared the mechanical properties of poly(vinyl acetate) (PVAc) filled with very find silica particles and with silica synthesized *in situ* by the sol–gel method. In the former case, two peaks appeared in the tan $\delta$ versus temperature spectrum. One corresponded to the glass transition of PVAc (*ca.* 60 °C), while the other was located at *ca.* 100 °C. Although this finding was not discussed extensively, it was thought that the second peak was due to motions of PVAc chains interacting with the silica particles.

At this point, it is important to recognize that surface–polymer interactions are essential not only for understanding the behavior of polymers containing filler particles but also for determining the structure and properties of solid or liquid polymeric thin films confined to molecular dimensions by solid surfaces. Such investigations are useful to a variety of practical applications, most notably lubrication and adhesion. In these systems, it is observed that an interphase between the wall and the bulk polymer film exists. The properties of the polymer chains forming the interphase deviate significantly from their corresponding values in the bulk.

Sokolov *et al.*[21] showed that the diffusion coefficient $D^*$ of polystyrene chains deposited as a 50 Å thick film on silicon wafers, was 1–2 orders of magnitude smaller than that of bulk polystyrene. Granick and co-workers[22] measured the response to shear of thin silicone films confined between two mica surfaces. They observed two different responses depending on the film thickness. When the film was thinner than 50 Å, the response was characterized as solid-like, since a critical shear strength had to be exceeded for the sliding motion to occur. For a film thickness larger than 50 Å, the response was liquid-like. No critical shear stress was required to activate sliding motion. A similar transition from solid-like to fluid-like behavior was observed for small molecule liquids such as hexadecane, but it took place at a smaller film thickness (27 Å). Furthermore, it was observed that although films thicker than 50 Å exhibited liquid-like behavior, their effective viscosity was 2–3 orders of magnitude higher than the bulk liquid viscosity. Schüller *et al.*[23] studied by dielectric spectroscopy the glass transition of propylene glycol and two poly(propylene glycol) samples of different molecular weights, which were confined in the pores (100 Å diameter) of a glass. The $T_g$ and the relaxation time were increased relative to those of the bulk samples. In addition, a new relaxation event was observed at a higher temperature for the confined materials, which was associated with a layer of molecules adsorbed at the surface of the pores. Molecular dynamics simulations that were designed to study the structure and dynamics of liquids at interfaces were in agreement with the experiments.[24] They showed that the density of the first and second liquid layers next to the surface are higher than the bulk density, resulting in an extreme crowding in the first layer, which leads to long relaxation times.

Although the solid–liquid or solid–polymer systems discussed above seem to be completely different, their properties stem from the same phenomenon, namely the dramatic reduction in mobility experienced by the segments of the liquid or polymer interacting with the solid surface. This may be due to entropy effects, local ordering or crowding at the interface. In a recent communication,[25] we reported that the regions of restricted mobility present in a wide range of polymers filled with very fine silica particles exhibit their own glass transition, as shown by the appearance of two peaks in their loss tangent curves. The first peak was due to the ordinary glass transition of the polymer, while the second was assigned to the glass transition of regions of restricted mobility. Comparison of the loss tangent curves of the filled polymers with corresponding random ionomer data revealed several striking similarities between the two systems. In both sets of materials, the height of the first peak is smaller than the height of the corresponding peak in pure homopolymers; the second peak was found to be located 60–100 deg higher than the first peak, and it was significantly broader. Furthermore, the activation energy of the second peak was lower than that of the first peak for both the ionomers and the filled polymers. The conclusion drawn from the above comparison was that ionomers and filled polymers probably share some dynamical and morphological features. Since regions of restricted mobility exist in filled polymers, they should exist also in ionomers, in agreement with the predictions of the EHM model.

Here, we wish to report the results of an examination of the dynamic mechanical properties of a variety of filled polymers, ranging from silicones to polystyrene, and to show that they exhibit two tan $\delta$ peaks, reflecting

**Table 1. Polymers, Their Average Molecular Weights, and the Source They Were Obtained from**

| polymer | abbreviation | MW | source |
|---|---|---|---|
| poly(vinyl acetate) | PVAc(LMW)[a] | 2 200[b] | synthesized |
| poly(vinyl acetate) | PVAc(MMW)[a] | 45 000[b] | Aldrich |
| poly(vinyl acetate) | PVAc(HMW)[a] | 121 000[b] | synthesized |
| polystyrene | PS | 200 000[c] | Polysciences |
| poly(methyl methacrylate) | PMMA | 350 000[c] | Polysciences |
| poly(4-vinylpyridine) | P4VP | 250 000[c] | SP2 |
| poly(dimethylsiloxane)[e] | PDMS | 360 000[b] | Dow-Corning |
| styrene–butadiene–rubber[f] | SBR | 200 000[d] | SP2 |
| poly[styrene–2.0 mol % 4-vinylpyridine] | P(S-2%VP) | ≈500 000[b] | synthesized |
| poly[styrene–5.6 mol % 4-vinylpyridine] | P(S-6%VP) | ≈500 000[b] | synthesized |
| poly[styrene–8.4 mol % 4-vinylpyridine] | P(S-8%VP) | ≈500 000[b] | synthesized |
| poly[styrene–11.5 mol % 4-vinylpyridine] | P(S-11%VP) | ≈500 000[b] | synthesized |

[a] LMW, MMW, and HMW: low, medium, and high molecular weight, respectively. [b] Number average molecular weight determined by GPC. [c] Weight average molecular weight, as reported by the supplier. [d] Viscosity average molecular weight, as reported by the supplier. [e] The sample is a copolymer of dimethyl (93 mol %) and methylphenyl (7 mol %) monomer units. The phenyl groups inhibit the crystallization of the polymer. [f] NMR measurements showed that the sample consists of 30 mol % styrene, 57 mol % 1,4-butadiene, and 13 mol % 1,2-butadiene units. Infrared measurements indicated that *ca.* 10% of the 1,4-butadiene units are in the *cis* conformation. Crystallization does not occur due to the high level of styrene units.

the presence of two glass transitions. Several factors affecting this behavior of filled polymers are studied. In particular, the effects of filler content, heat treatment, and molecular weight on the tan $\delta$ curves are investigated in detail for poly(vinyl acetate). The effect of varying the number of monomer units which interact strongly with the silica particles, is studied for styrene–4-vinylpyridine copolymers. Finally, a morphological model is proposed in order to account for these experimental observations.

## Experimental Section

The various polymers used, their sources, and their average molecular weights are reported in Table 1. The reported MW of the polymers obtained commercially are those reported from the manufacturers. The silica particles (Aldrich) used as filler were 7 nm in nominal diameter with a specific surface area of 380 $m^2/g$.

The synthesis of PVAc(LMW), PVAc(HMW), and P(S-*X*%VP) samples was carried out by bulk free radical polymerization, with benzoyl peroxide as initiator, at 70 °C. The molecular weight of the polymers was measured with GPC, using polystyrene standards and THF as solvent. The small 4-vinylpyridine content of the P(S-*X*%VP) samples did not affect significantly the GPC analysis. The 4VP content in these polymers was determined by infrared spectroscopy. The bands at 1555 and 1414 $cm^{-1}$ are associated with 4-vinylpyridine content, while the bands at 1945 and 1875 $cm^{-1}$ are ascribed to styrene units. The calibration curves constructed by Smith *et al.*[26] using these assignments were also used here.

In a typical preparation of a polymer filled with silica particles, 4 g of the polymer were dissolved in 50 mL of THF or DMF in the case of poly(4-vinylpyridine). Then the proper amount of silica particles was added, and the solution was stirred for 48 h. Following evaporation at room temperature under stirring, the polymer was dried in a vacuum oven at 110 °C for 24 h. It was later used to prepare samples for dynamic mechanical measurements. Some of the samples were subjected to additional heat treatment at 180 °C for 12 h under vacuum, as will be indicated when describing the results.

A Polymer Laboratories dynamic mechanical thermal analyzer was used to measure the mechanical properties of the samples as a function of temperature for five frequencies (0.3, 1, 3, 10, and 30 Hz). The tan $\delta$ versus temperature spectra were fitted with an exponential background and exponentially modified Gaussians (EMG) in order to obtain peak positions and peak areas. These functions were selected because they provided reasonable fits to the data on filled polymers presented here as well as relevant data on poly(styrene–sodium methacrylate) ionomers.[8] The exponential background was needed to fit the upturn of the curve in unfilled polymers and was used for the filled polymers in order to maintain consistency. It should be noted, though, that if a linear background had been used in the case of filled polymers, the curve-fitting results would not have changed significantly. The shape of the tan $\delta$ peaks was approximated sucessfully with the EMG function, the appearance of which is that of a distorted Gaussian. It is asymmetric, with an exponential tail on the right side.[27] It fits well tan $\delta$ peaks due to a glass transition because it incorporates a variable degree of asymmetry. Several efforts to fit the data with pure Gaussian peaks were unsuccessful. Given the opportunity, it should be emphasized that to the best of our knowledge there is no theoretical justification for any specific function to be used to fit tan $\delta$ curves. Thus the following criteria were used to determine the acceptability of the fits: (a) Do not use more peaks than the data provide evidence for. (b) Be consistent; use the same functions for all data, so comparisons will be meaningful. (c) Do not accept unrealistic peak shapes, like EMG peaks with long tails due to large asymmetries. As in the case of random ionomers, activation energies were obtained from the peak positions and the volume fraction of the material associated with a particular glass transition was estimated from the peak areas. A Perkin-Elmer IR-16 instrument was used for the infrared measurements. The morphology of the silica particles in different polymers was observed by TEM.

## Results

**I. Generality of the Second Transition.** In order to investigate the effect of increasing the filler content on the dynamic mechanical properties of several polymers, samples of PS, SBR, PDMS, and P4VP containing various amounts of silica particles (7 nm diameter) were prepared. This range of polymers is thought to be necessary if the generality of the earlier observed phenomena, namely the existence of a second glass transition in filled polymers, is to be established. The tan $\delta$ curves measured at 0.33 Hz are presented in Figure 1 for two filler contents, while the associated numerical results, obtained by curve fitting, are reported in Table 2. The tan $\delta$ curves are plotted vs $T - T_g$ ($T_g$ being the maximum of the first peak) for reasons of comparison and clarity. In order to consolidate all the relevant results in a single graph, a logarithmic scale for the tan $\delta$ axis was used; hence the observed peaks appear to be broader and less intense when Figure 1 is compared with the corresponding linear plots of our previous publication.[25] It is observed that at silica contents at or above 10 wt % (20 wt % for PDMS), all the samples exhibit two tan $\delta$ peaks. The first peak, found at the $T_g$ of the unfilled polymer, corresponds to the usual glass transition. The position of this peak remains unchanged as the filler content increases, but

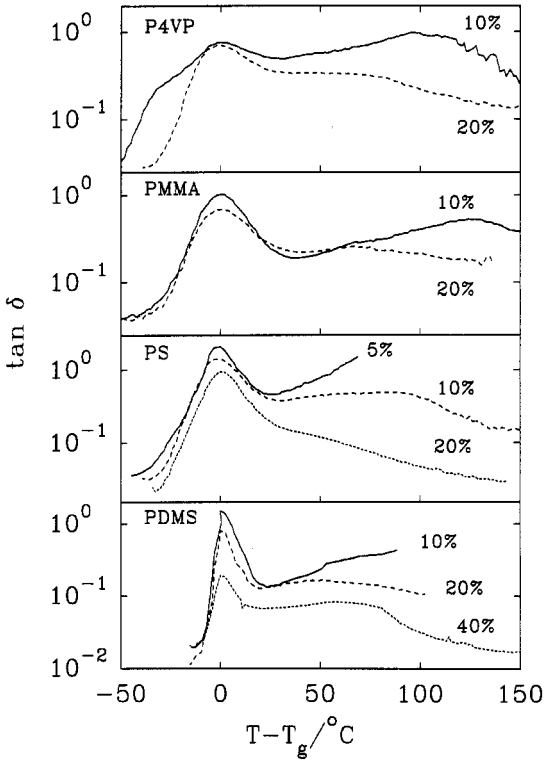


**Figure 1.** Semilog plot of tan $\delta$ versus $(T - T_g)$ curves for PDMS, PS, PMMA, and P4VP composites, containing different amounts of silica particles.

**Table 2. Results of the Mechanical Measurements (tan $\delta$ − 0.33 Hz) of Various Polymers[a]**

| polymer | wt % $SiO_2$ | $T_{g_1}$/ °C | $T_{g_2}$/ °C | $area_1$ | $area_2$ | $E_{a_1}$/ kJ·mol$^{-1}$ | $E_{a_2}$/ kJ·mol$^{-1}$ |
|---|---|---|---|---|---|---|---|
| PDMS | 10 | −105 | | | | | |
| PDMS | 20 | −102 | −57 | 6 | 11 | 240 | 140 |
| PDMS | 40 | −106 | −53 | 2 | 5 | 210 | 150 |
| SBR | 0 | −22 | | 19 | | 260 | |
| SBR | 20 | −3 | 41 | 19 | 22 | 290 | 280 |
| SBR | 30 | −8 | 33 | 9 | 15 | 230 | 260 |
| PS | 0 | 110 | | 58 | | 520 | |
| PS | 10 | 104 | 176 | 31 | 42 | 480 | 130 |
| PS | 20 | 106 | 144 | 21 | 6 | 600 | 200 |
| P4VP | 10 | 140 | 235 | | | | |
| P4VP | 20 | 137 | 199 | 21 | 23 | | |
| PMMA | 10 | 100 | 222 | | | | |
| PMMA | 20 | 93 | 160 | | | | |

[a] Curve fitting of tan $\delta$ curves was performed for some of the samples. The parameters obtained are the positions ($T_g$) and the areas of the peaks. The activation energies ($E_a$) of the transitions were calculated from the frequency dependence of the peak positions.

its size decreases. This is an indication that the fraction of chains participating in the glass transition decreases as the composite becomes richer in silica particles. The second peak is broader than the first and, depending on the polymer, is located 40−110 deg higher than the first. As the particle content increases, the size of the peak decreases, while its maximum shifts to a lower temperature. From the frequency variation of the peak maximum, the activation energy of both tan $\delta$ peaks can be calculated. The results (Table 2) show that the activation energy of the first peak is not affected, within experimental error, by the incorporation of silica particles into the polymers. The activation energy of the second tan $\delta$ peak is lower than that of the first peak, but it is still significant. On the basis of its position and activation energy, the second tan $\delta$ peak is assigned to the glass transition of polymer chains experiencing

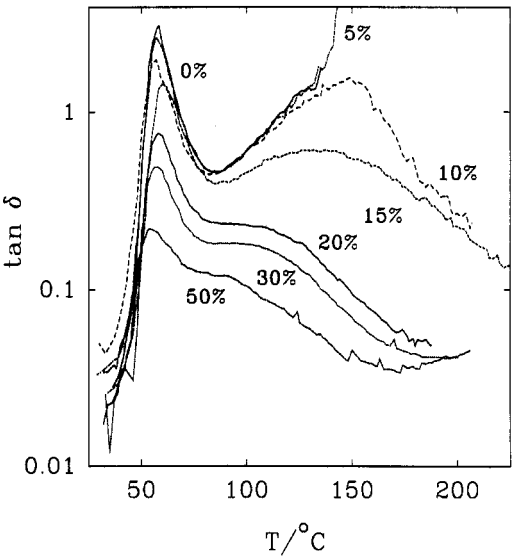


**Figure 2.** Semilog plot of tan $\delta$ versus temperature curves for PVAc composites, containing different amounts of silica particles. Only the first runs are shown for each sample.

mobility restrictions due to interactions with the filler particles. The above observations are in good agreement with our earlier results[25] as well as the results of others and support the interpretation of ionomer properties based on the EHM morphological model. Also, the presence of a second tan $\delta$ peak accompanying the incorporation of silica particles, in the curves of such different polymers as those examined, supports the generality of the notion that polymer chains of restricted mobility are capable of exhibiting their own glass transition, at a temperature higher than that of the matrix polymer. An explanation, though, is still needed for the size decrease and position shift of the second peak with increasing silica content.

**II. Factors Affecting the Second Transition.** *PVAc Samples.* In order to examine in greater detail the effect of increasing filler content on the dynamic mechanical properties of the host polymer, the tan $\delta$ versus temperature curves of medium molecular weight PVAc samples ($M_n$ = 45 000) containing different amounts of silica were measured and are presented in Figure 2. The corresponding numerical results obtained by the curve fitting are found in Table 3. It is observed that as the silica content increases, the height of the peak at *ca.* 60 °C, which corresponds to the PVAc glass transition, gets smaller. This is an indication that some of the polymer chains do not participate in this transition. Furthermore, a second peak is observed at higher temperatures for samples containing 10 wt % or more silica. The position of the peak maximum shifts to lower temperatures and the peak size decreases as the silica content increases. Both peaks exhibit a significant frequency dependence, from which the activation energy of the transitions is calculated.

In addition to the above results, it was also found that the mechanical properties of PVAc samples containing less than 20 wt % silica depended on heat treatment. The loss tangent curves obtained from a second or a third run differed significantly from that of the first run. In Figure 3, the tan $\delta$ versus temperature curves, measured at three successive runs for a PVAc sample containing 12.5 wt % silica, are shown. While very little change is noted for the position and size of the first peak, the position of the second shifts to a lower temperature and becomes smaller when the tan $\delta$ of the

**Table 3. Results of the Curve-Fitting Process of the PVAc (MMW) tan δ Curves, Measured at 0.33 Hz[a]**

| wt % $SiO_2$ | $T_{g_1}$/ °C | $T_{g_2}$/ °C | area$_1$ | area$_2$ | $E_{a_1}$/ kJ·mol$^{-1}$ | $E_{a_2}$/ kJ·mol$^{-1}$ |
|---|---|---|---|---|---|---|
| 10.0 (not annealed) | 58 | 156 | 35 | 99 | 340 | 240 |
| 10.0 (2nd run) | 59 | 144 | 27 | 57 | 350 | 110 |
| 12.5 (not annealed) | 61 | 161 | 27 | 88 | 360 | 150 |
| 12.5 (2nd run) | 60 | 143 | 25 | 58 | 350 | 120 |
| 12.5 (3rd run) | 60 | 133 | 24 | 45 | 350 | 120 |
| 12.5 (annealed) | 60 | 137 | 22 | 46 | 340 | 120 |
| 12.5 (2nd run) | 60 | 134 | 25 | 45 | 360 | 130 |
| 12.5 (3rd run) | 60 | 128 | 25 | 42 | 360 | 110 |
| 15.0 (not annealed) | 60 | 140 | 26 | 55 | 340 | 150 |
| 15.0 (2nd run) | 61 | 140 | 25 | 52 | 370 | 160 |
| 15.0 (3rd run) | 60 | 130 | 21 | 37 | 350 | 130 |
| 17.5 (not annealed) | 61 | 135 | 23 | 43 | 350 | 210 |
| 17.5 (2nd run) | 61 | 126 | 20 | 29 | 360 | 150 |
| 17.5 (3rd run) | 60 | 120 | 19 | 23 | 360 | 140 |
| 17.5 (annealed) | 58 | 115 | 20 | 25 | 360 | 140 |
| 17.5 (2nd run) | 60 | 121 | 19 | 22 | 340 | 140 |
| 17.5 (3rd run) | 60 | 113 | 19 | 19 | 350 | 150 |
| 20.0 (not annealed) | 60 | 107 | 13 | 14 | 350 | 350 |
| 30.0 (not annealed) | 60 | 106 | 9 | 10 | 350 | 460 |
| 40.0 (not annealed) | 58 | 103 | 7 | 9 | 380 | 320 |
| 50.0 (not annealed) | 56 | 95 | 4 | 4 | 420 | 240 |

[a] The parameters obtained are the positions ($T_g$) and the areas of the peaks. The activation energy ($E_a$) of the transitions were calculated from the frequency dependence of the peak positions. The thermal history of each sample is indicated in parentheses in the first column. The annealing procedure consisted of 12 h of heating under vacuum at 180 °C. The run number refers to consecutive runs on the same sample without removing it from the DMTA apparatus.

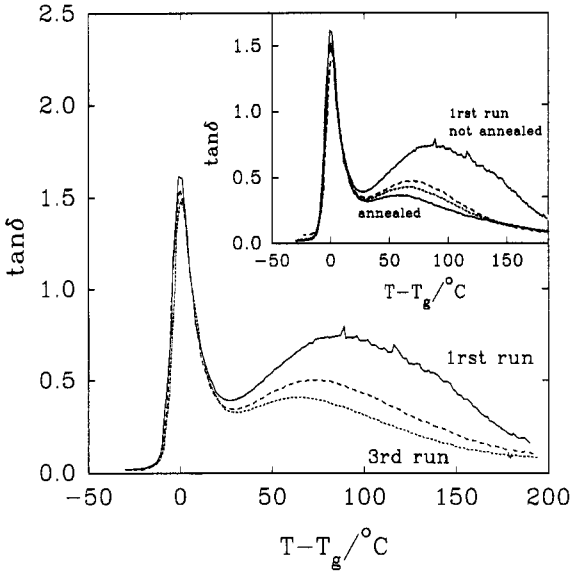


**Figure 3.** Main graph: tan δ versus ($T - T_g$) curves for three successive runs on a PVAc composite containing 12.5 wt % silica. Inserted graph: tan δ versus ($T - T_g$) curves for the first run of the not annealed PVAc composite containing 12.5 wt % silica and three successive runs of an annealed sample of the same composition.

sample is measured for a second or third time. Similar behavior is observed when the sample is annealed at 180 °C for 12 h under vacuum. These results are shown in the inserted graph in Figure 3, where three successive runs of the annealed sample are compared with the very first run of the unannealed sample. PVAc samples containing 10, 15, and 17.5 wt % silica behaved in the same manner. However the effects of heat treatment on the tan δ curves became weaker as the silica content increased and finally, at 20 wt %, were not observed at all.

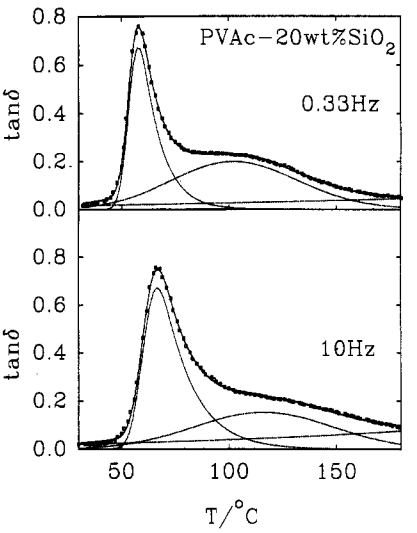


**Figure 4.** Representative results of the curve-fitting process for a PVAc composite containing 20 wt % silica, at 0.33 and 10 Hz. The results also illustrate the frequency variation of the tan δ curves.

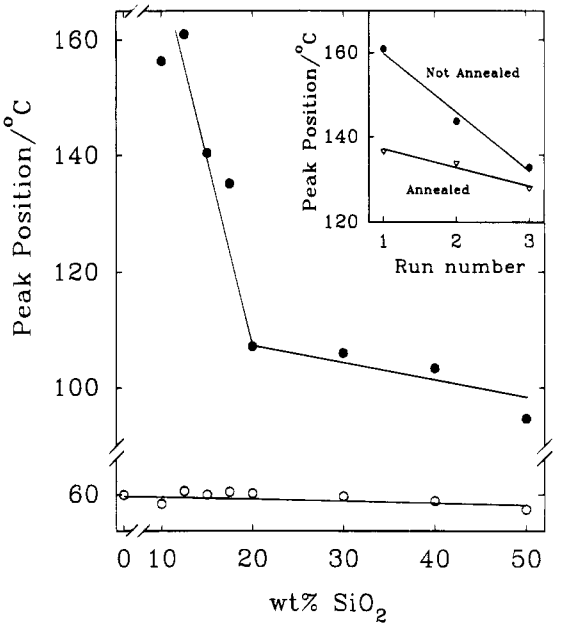


**Figure 5.** Main graph: Peak position of the first (○) and the second (●) tan δ peaks versus silica content for the PVAc composites. Inserted graph: Peak position of the second peak versus run number for a not annealed (●) and an annealed (▽) PVAc composite containing 12.5 wt % silica. The lines in both graphs serve as a guide to the eye.

Quantification of the effects of increasing the silica content and of annealing on the mechanical properties of PVAc was achieved by fitting the tan δ curves with an exponential background and two exponentially modified Gaussian bands. Representative results of the curve-fitting process are shown for the tan δ curves of PVAc/20 wt % silica, measured at 0.33 and 10 Hz, in Figure 4. From this treatment of the data, the area under each peak is obtained as well as the peak maximum. When the latter is plotted as a function of frequency in an Arrhenius type plot, the activation energy of each glass transition is calculated. These results are reported in Table 3. The position of the two peaks is plotted against the silica content in Figure 5. The position of the first tan δ peak, due to the usual polymer glass transition, remains constant at 59 ± 2 °C, while that of the second tan δ peak exhibits a

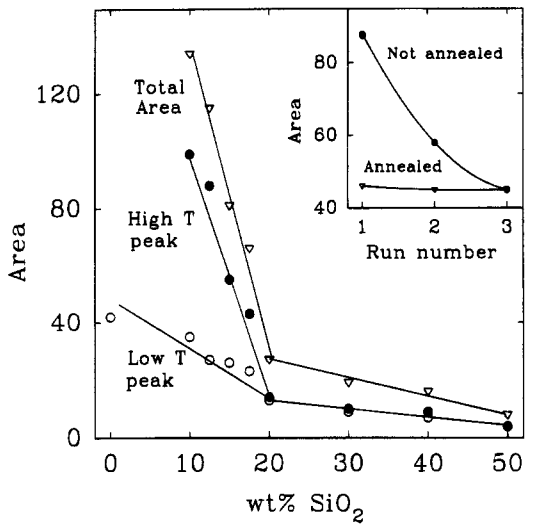


**Figure 6.** Main graph: Area of the first (○) and the second (●) tan $\delta$ peak as well as total area (▽) versus silica content for the PVAc composites. Inserted graph: Area of the second tan $\delta$ peak versus run number for a not annealed (●) and an annealed (▽) PVAc composite containing 12.5 wt % silica.

significant variation. It decreases rapidly from *ca.* 160 °C to *ca.* 110 °C between 10 and 20 wt % silica content. The decrease continues for the samples containing more than 20 wt % silica, but at a slower rate. The thermal history of the sample does not affect the position of the first peak, but as shown in Figure 5 (inserted graph), it has a significant effect on that of the second peak, which for all samples examined, decreases as the tan $\delta$ is measured for a second or a third time on the same specimen.

The second parameter to be examined is the area of the two peaks. In Figure 6, where the peak area is plotted as a function of silica content, it is observed that the area of the first peak decreases by 1 order of magnitude when the filler content increases from 0 to 50 wt %. The decrease is fast in the 0–20 wt % region, but is slower above 20 wt % silica. This trend indicates that fewer polymer chains participate in the glass transition. The area under the second peak decreases rapidly by a factor of 10 from 10 to 20 wt % silica content and then decreases with the same rate as the area of the first peak. For samples containing more than 20 wt % silica, the areas of the two peaks are equal. Thermal history affects the area of the second peak, which decreases as repeat measurements are performed on the same specimen. The activation energy of the first transition remains constant (*ca.* 350 kJ/mol) up to 30 wt % silica and then increases to *ca.* 400 kJ/mol at 50 wt % silica. In the case of samples containing less than 20 wt % silica, the activation energy of the second transition is *ca.* 200 kJ/mol, significantly smaller than that of the first. Then it increases, and for the sample containing 30 wt % silica, the activation energy of the second transition is *ca.* 500 kJ/mol, which is higher than that of the first. For still higher filler contents, it decreases and becomes smaller than that of the first transition, reaching *ca.* 250 kJ/mol at 50 wt % silica. Thermal history does not have a major effect on the activation energy of the two transitions. The activation energy of the first transition is unaffected, while that of the second transition decreases somewhat as more measurements are performed on the same specimen.

Another important parameter affecting the polymer properties is the average molecular weight. The tan $\delta$

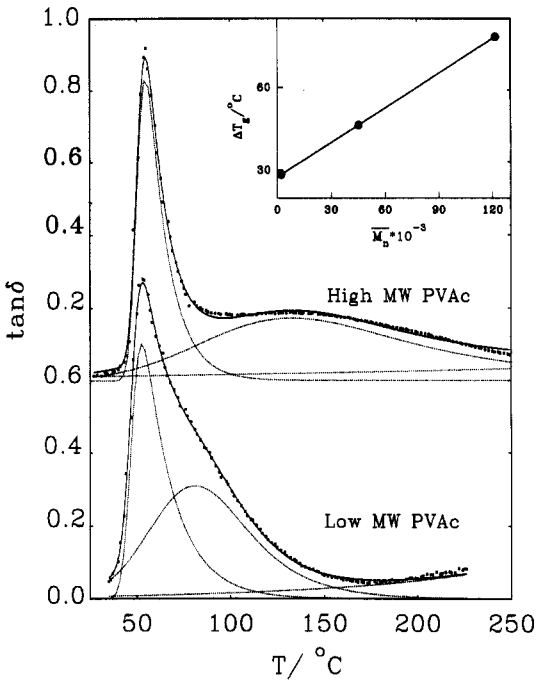


**Figure 7.** Main graph: tan $\delta$ versus temperature curves for PVAc of low (4500) and high (122 000) MW, containing 20 wt % silica, along with the corresponding curve-fitting results. Inserted graph: $\Delta T_g$ versus number average molecular weight for PVAc composites containing 20 wt % silica.

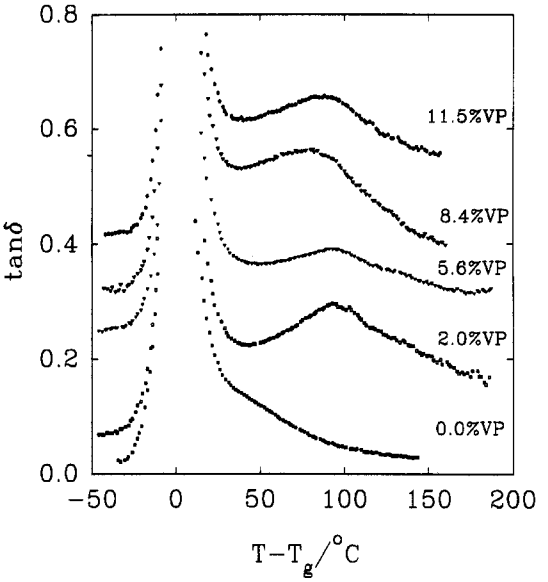


**Figure 8.** tan $\delta$ versus ($T - T_g$) for styrene–4-vinylpyridine copolymers of different VP contents, but containing 20 wt % silica.

curves for three PVac samples of low MW ($M_n$ = 2200), medium MW ($M_n$ = 45 000), and high MW ($M_n$ = 121 000), all containing 20 wt % silica particles, were measured in order to evaluate the effect of molecular weight on the two glass transitions. The actual tan $\delta$ curves, along with the corresponding results of the curve-fitting process for the lowest and highest MW samples, are shown in Figure 7. The position and the size of the first peak is not affected by the molecular weight increase. The position of the second peak, though, shifts to a higher temperature as the MW increases. As shown in the inserted graph in Figure 8, the difference between the two glass transition temperatures, $\Delta T_g$, varies linearly with the number average molecular weight of the polymer. This trend indicates

**Table 4. Results of the Curve-Fitting Process of the Styrene–Vinylpyridine Copolymers tan δ Curves, Measured at 0.33 Hz[a]**

| wt % $SiO_2$ | mol % 4VP | $T_{g_1}$/ °C | $T_{g_2}$/ °C | $\Delta T_g$/ °C | $area_1$ | $area_2$ | $E_{a_1}$/ kJ·mol$^{-1}$ | $E_{a_2}$/ kJ·mol$^{-1}$ |
|---|---|---|---|---|---|---|---|---|
| 0 | 0.0 | 110 | | | 58 | | 520 | |
| 0 | 2.0 | 118 | | | 56 | | 520 | |
| 0 | 5.6 | 118 | | | 42 | | 540 | |
| 0 | 8.4 | 110 | | | 44 | | 480 | |
| 0 | 11.5 | 119 | | | 40 | | 510 | |
| 10 | 0.0 | 104 | 176 | 72 | 31 | 42 | 480 | 130 |
| 10 | 2.0 | 117 | 215 | 98 | 30 | 41 | 560 | 230 |
| 10 | 5.6 | 112 | 231 | 119 | 35 | 36 | 510 | 290 |
| 10 | 8.4 | 119 | 224 | 105 | 30 | 61 | 540 | 140 |
| 10 | 11.5 | 114 | 216 | 102 | 30 | 68 | 520 | 170 |
| 20 | 0.0 | 106 | 144 | 38 | 21 | 6 | 600 | 200 |
| 20 | 2.0 | 113 | 203 | 90 | 23 | 24 | 540 | 190 |
| 20 | 5.6 | 113 | 202 | 89 | 22 | 12 | 510 | 320 |
| 20 | 8.4 | 115 | 185 | 70 | 22 | 26 | 530 | 230 |
| 20 | 11.5 | 112 | 191 | 79 | 22 | 20 | 500 | 300 |
| 30 | 0.0 | | | | | | | |
| 30 | 2.0 | 107 | 170 | 63 | 12 | 6 | 560 | 250 |
| 30 | 5.6 | 109 | 195 | 86 | 15 | 4 | 520 | 470 |
| 30 | 8.4 | 117 | 154 | 37 | 9 | 10 | 530 | 320 |
| 30 | 11.5 | 112 | 152 | 40 | 9 | 10 | 540 | 350 |

that longer polymer chains experience stronger mobility restrictions than shorter chains. This is in qualitative agreement with the theoretical prediction of Kosmas,[28] who showed that the average number of contacts between a polymer chain and a surface is proportional to the square root of the molecular weight of the polymer. Thus, the longer the polymer chain, the larger the number of adsorbed segments will be and consequently the stronger the mobility restrictions. On the other hand, longer chains have a higher probability of adsorbing to two different particles, constituting bridges between the particles. However, the mobility of bridging chains is lower than that of nonbridging chains, hence the former have a higher $T_g$.

*Styrene–Vinylpyridine Copolymers.* Copolymers of styrene and 4-vinylpyridine (VP) were filled with silica particles, and their dynamic mechanical properties were measured. The presence of pyridine groups should enhance the polymer–filler interactions through the acid–base mechanism operating between silanol groups on the particle surface and pyridine groups on the polymer chains. Detailed studies of such interactions between various polymers and several particulate substrates can be found in the work of Schreiber and coworkers.[29] Due to the strengthening of the polymer–filler interactions, the second peak in the tan δ curves of the copolymers is expected to be significantly affected when compared with the second peak of homopolystyrene containing the same amount of silica. On the other hand, there should be little effect, if any, on the first peak.

The tan δ versus $(T - T_g)$ curves for samples containing 0–11.5 mol % VP, filled with 20 wt % silica particles, are presented in Figure 8. The corresponding numerical results of curve-fitting are reported in Table 4. A small increase in the first glass transition temperature is observed when VP is copolymerized with styrene due to the copolymerization effect. The size of the peak and the activation energy of the transition are not affected by the introduction of small amounts of VP into the polymer backbone. Significant effects, though, can be noticed in connection with the second glass transition. The difference between the two glass transition temperatures, $\Delta T_g$, increases by 30–50 deg, when VP groups are part of the polymer chains, and the area of

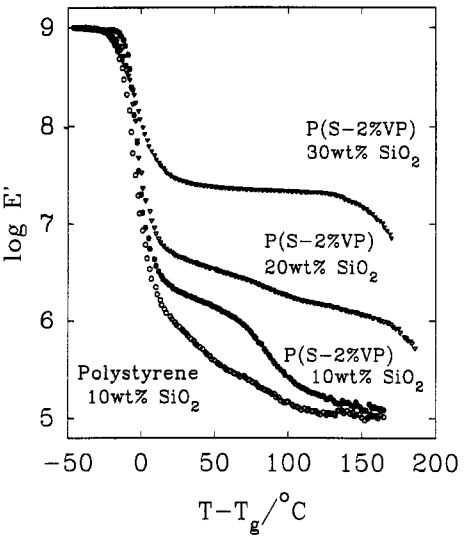


**Figure 9.** log $E'$ versus $(T - T_g)$ for PS containing 10 wt % silica and for P(S-2%VP) containing different amounts of silica.

the second peak is 2–4 times larger for the VP copolymers than for homopolystyrene. The activation energy of the second peak is lower than that of the first for all the samples. The shift of the second peak to higher temperatures indicates that the strength of the interactions between styrene–VP copolymers and silica is higher than that of pure polystyrene and silica. Consequently, it reinforces the assignment of the second tan δ peak to the glass transition of polymer chains whose mobility is restricted by interactions with the filler particles.

In Figure 9, the log $E'$ versus temperature curves are presented for PS containing 10 wt % silica and P(S-2%VP) containing 10, 20, and 30 wt % silica. A sharp drop of the modulus is observed at the first glass transition for all the samples. The magnitude of the drop depends on the filler content; it is the smallest for the sample containing 30 wt % silica, which, as expected, exhibits the largest reinforcement. At temperatures higher than the $T_g$, each sample behaves differently. The modulus of the PS composite decreases slowly from $T_g$ to $T_g$ + 150 °C. The P(S-2%VP) sample containing 10 wt % silica exhibits a plateau-like region at $E' \approx 10^6$ Pa for temperatures between $T_g$ and $T_g$ + 75 °C. A second drop of the modulus appears at $T_g$ + 75 °C, signifying the second glass transition. The sample containing 20% silica exhibits similar features, but the modulus value at the plateau region is higher and the second drop of the modulus is very small. Finally, in the case of the P(S-2%VP) composite containing 30 wt % silica, the plateau persists to high temperatures. A plateau-like region in the modulus at temperatures between the two glass transitions is observed for most of the composites. However, the second drop of the modulus is observed only for some PMMA, P4VP, P(S-2%VP), and P(S-5.6%VP) composites, but not for PS or PVAc composites.

*Morphology.* Transmission electron micrographs are presented in Figure 10 for PVAc and P(S-11%VP), containing 20 wt % silica. The photographs show that both samples are heterogeneous, as expected. In the case of PVAc, it is calculated that the diameter of the smaller single particles is 50–100 nm, indicating that the inorganic phase consists of highly aggregated particles. Actually, the picture reveals that a network of particles is formed, and the boundaries between the

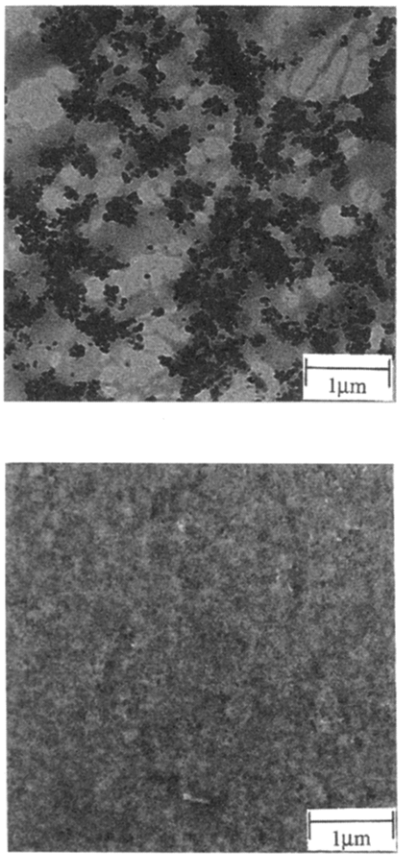


**Figure 10.** TEM micrographs of (a) PVAc and (b) P(S-11.5%VP) containing 20 wt % silica.

silica phase and the PVAc phase are readily distinguishable. These observations are in agreement with the results of Landry *et al.*[20] The morphology of the filled styrene–vinylpyridine copolymer appears to differ from that of the PVAc sample; the silica particles seem to be homogeneously distributed throughout the material, as shown in Figure 10b. Since polystyrene composites have the same morphology as those based on PVAc, we believe that the reason for the different morphology of the styrene–vinylpyridine copolymer composites lies in the strong acid–base interactions between silica and VP. The strength of these interactions may lead to the disruption of large aggregated particle structures and the intimate mixing of the two phases. A similar argument was proposed by Landry *et al.*[20] to explain similar differences between the morphologies of PVAc filled with silica particles and PVAc filled with silica formed *in situ* by the sol–gel method. The larger amount of silanol groups on the surface of the sol–gel silica leads to an increase of the number of hydrogen bonds between the inorganic and polymer phases, causing their intimate mixing. Our interpretation is also in accord with the mechanical measurements described earlier. The $\Delta T_g$ for the 20 wt % silica-containing PS sample is 47 deg, while for the corresponding P(S-11%VP) sample it is 79 deg. This difference reflects the large difference between the particle–polymer interactions in the two composite materials.

## Discussion

The dynamic mechanical study of filled polymers undertaken here has been motivated by the desire to investigate the effects of chain mobility restrictions on the glass transition in these systems. Specifically, it was of great interest to search for similarities between filled polymers and random ionomers and to examine whether the mobility restrictions could be related to the presence of a second glass transition, as has been proposed in the EHM model for random ionomers. Indeed, the work published earlier and the results presented here have revealed many similarities between the mechanical properties of random ionomers and those of filled polymers. In this respect, an important outcome of this study is the establishment of the generality of the second tan $\delta$ peak. The peak appeared in a wide variety of polymers (PDMS, SBR, PVAc, PMMA, PS, P4VP), although its detailed characteristics depended on several factors, including the nature of the polymer, filler content, polymer MW, and thermal history. The high specific surface area (SSA) of the particles was shown to be essential for the appearance of the second glass transition.[25] The new peak appeared in the case of very fine particles (SSA $\approx$ 380 $m^2/g$), but no effect was observed when large particles (SSA $\approx$ 1 $m^2/g$) were used. The primary fine particles (7 nm diameter) appeared to be agglomerated, with the smallest of the aggregates being *ca.* 50 nm in diameter, as measured from the TEM pictures. The assignment of the second tan $\delta$ peak as the glass transition of chains experiencing mobility restrictions was based on the peak position and its high activation energy. Moreover, the molecular weight dependence exhibited by the second tan $\delta$ peak was in agreement with this assignment. Longer chains are expected to experience mobility restrictions stronger than shorter chains, because the probability of their being a bridge between two particles is higher. The assignment was further reinforced by the styrene–vinylpyridine results. The $\Delta T_g$ and the area under the second peak are larger for these copolymers than for homopolystyrene, because of the very strong silica–VP acid–base interactions. The generality of the second tan $\delta$ peak and its assignment to the glass transition of polymer chains of reduced mobility reinforce the idea that chain mobility restrictions can be so severe as to cause a new glass transition, thus arguing in favor of that aspect of the EHM model.

In the course of this work, a major difference between ionomers and filled polymers was found. Superficially, the incorporation of more particles in the case of filled polymers might be thought to correspond to an increase of the ion content in the case of ionomers. For styrene ionomers, the total area under the tan $\delta$ curves (sum of the areas of both peaks) is independent of the ion content, and the $\Delta T_g$ increases with increasing ion content. To our surprise, the trends for filled polymers were different. The total area and the $\Delta T_g$ both decrease with increasing particle content. These differences suggested that the morphological model for ionomers could not be adopted directly for filled polymers. Instead, a modification of that model, which involves a higher degree of complexity, was needed.

In order to understand the morphological and structural changes accompanying an increase of filler concentration in the composites, the schematic model of Figure 11 is proposed. The model incorporates the morphology of polymer chains around a filler particle described by McBrierty and coworkers,[14] coupled with the idea of overlapping restricted mobility regions, developed in the EHM model.[2] The model presents conceptually the sequence of events accompanying the incorporation of increasing amounts of silica particles

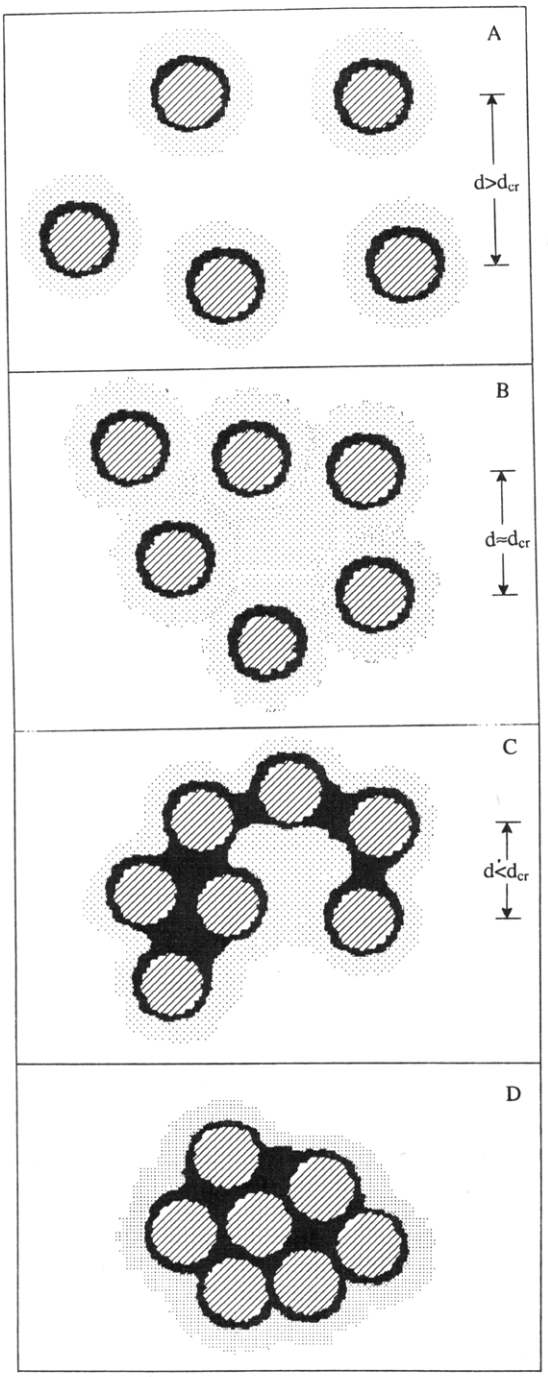


**Figure 11.** Schematic model of the morphological transformations in filled polymers, occurring as the silica content increases from less than 10 wt % (A), to ca. 10 wt % (B), to over 20 wt % (C), to over 50 wt % (D). The line-shaded areas are the silica particles, while the black areas correspond to tightly bound polymer and the gray areas to loosely bound polymer.

in the polymer, which results in a decrease of the average interparticle distance, $d$. Although it is considered useful for the following discussion to consider the increase of filler amount from one composition to the next as a continuous process, it should be kept in mind that sample preparation is a batch mode process. Consequently, the configuration and state of mobility of the polymer chains in a particular sample does not affect their state in another sample of lower or higher filler content.

The building unit of the model is the silica particle (indicated by line shading) surrounded by a layer of polymer (black areas), which appears to be immobile in the temperature and frequency regimes examined and thus does not participate in either of the two glass transitions. We will designate this part of the polymer as immobilized or tightly bound, in analogy to similar nomenclature found in the rubber literature. The original formation of the tightly bound polymer could be visualized as taking place through mechanisms involving multisegment adsorption. The configuration of the polymer chains in the immobilized state (random coil or loops and trains) has been discussed recently by Vilgis and Heinrich.[30] The polymer chains capable of participating in the second glass transition (gray areas) will be called polymer of reduced mobility or loosely bound polymer. As discussed in the Introduction, the existence of polymer chains in these states has been observed by NMR.[13-16] It should be recalled that according to the EHM model, the second glass transition is not observable unless the regions of restricted mobility overlap, since the dimensions of the individual regions are not large enough. The present model differs from the EHM model in the existence of tightly bound polymer chains. Ionic multiplets in styrene ionomers do not induce mobility restrictions on the attached chains severe enough to immobilize them completely. In addition, the location of the multiplets is not completely random throughout the matrix, in contrast to the location of filler particles, because the constituents of the multiplets, the ionic groups, are rigidly connected to the matrix polymer. Thus, the multiplets adopt a relatively narrower distribution of distances than that adopted by the filler particles.

When the silica content is much lower than 10 wt %, the average interparticle distance is large and the mobility of the polymer next to the immobilized layers is not significantly affected (Figure 11a); hence no new glass transition is observed, although the magnitude of the first glass transition decreases, signifying the formation of tightly bound polymer around the particles. Near 10 wt % silica, the average interparticle distance has a "critical" value, $d_{cr}$; the mobility of polymer chains located between particles with distance $d \leq d_{cr}$ is reduced. Thus, regions of a continuous phase of restricted mobility (light gray regions), which now are large enough to exhibit their own glass transition are formed (Figure 11b). The polymer in these regions will be called loosely bound. It should be emphasized at this point that the strength of the mobility restrictions is not uniform throughout the composite, since they are induced by a wide distribution of interparticle distances. As the average interparticle distance decreases further, with the incorporation of more filler particles, the mobility restrictions become so severe that the loosely bound polymer is gradually transformed to tightly bound (Figure 11c). Hence the volume fraction of loosely bound polymer decreases, resulting in a decrease in the area of the second tan $\delta$ peak; by contrast, the volume fraction of tightly bound polymer increases in parallel with the volume fraction of filler or perhaps even more strongly since bridging is important. This results in a further drop in the total area under the two tan $\delta$ peaks. As the interparticle distance decreases, it is the most restricted regions of loosely bound polymer (i.e. those with the highest $T_g$) which are transformed first into tightly bound polymer. Thus, the regions with the highest $T_g$ will be eliminated earliest as filler content increases, resulting in an actual decrease of the second $T_g$. Also, as more and more polymer is immobilized, the

more it screens the effect of the solid particles on loosely bound polymer. At low filler content, the amount of the immobilized polymer around the particles is small, allowing for sufficiently strong interactions between the loosely bound polymer and the particles. As the amount of immobile polymer increases at higher filler contents, such interactions become progressively weaker. Hence, since the immobile polymer does not restrict the chain mobility as efficiently as the solid particles, the second $T_g$ decreases. Finally, at very high filler content, the average interparticle distance is much smaller than $d_{cr}$, and nearly all the polymer chains are immobilized (Figure 11d).

Two fundamental postulates constitute the basis of the proposed model. The first suggests that in order for the second glass transition to be observed, overlap of the regions of loosely bound polymer is needed, which for all polymers except PDMS is achieved at 10 wt % silica. To explain this exception, which, as will become clear, verifies the postulate, it is important to realize that silicones, due to the unrestricted motion of the methyl groups, are characterized by larger interchain distances than carbon-based polymers, which is probably reflected in a lower persistence length.[31] Thus, it takes more silica particles to induce overlap of the regions of restricted mobility, than in the other polymers examined. This behavior is also in agreement with the results on PDMS–carboxylate random ionomers.[32] It was observed that the ionic content should be higher than 8 mol % for the second glass transition to appear in these polymers, in sharp contrast with the corresponding styrene ionomers, where the second glass transition appears at *ca.* 2 mol % ionic content.[8] The second postulate that the model is based on suggests that the immobile polymer is not as efficient as the solid particles in restricting the mobility of the loosely bound polymer. This is supported by the results of Kraus and co-workers[33] on the mechanical properties of SBR filled with PS particles. Although the modulus in the rubbery state increased with the incorporation of more PS particles, signifying reinforcement of the rubber by the filler, no second tan $\delta$ peak appeared which could be attributed to the rubber phase. This appears to suggest that the PS particles could not restrict the mobility of polymer chains beyond those of the immobile layer.

The thermal history was found to affect the mechanical properties of polymer samples containing 10–20 wt % silica. Both the peak position and the area of the second tan $\delta$ peak decreased with prolonged thermal treatment. Physical aging or annealing effects have been observed before in a number of cases.[9] It has also been observed that the density of filled polymers increases during annealing, the effect diminishing as the filler concentration increases. This means that during the formation of the composite, excess free volume is created, which later relaxes gradually. Ito and co-workers[16] noticed that during annealing, loosely bound rubber is transformed to tightly bound rubber. This may account for the density increase, since it has been established that the density of the polymer layer adsorbed on a surface is a few percent higher than the density of the bulk polymer.[34] Our results are in agreement with the above observations. The area of the second tan $\delta$ peak decreases with annealing, while the area of the first peak does not change significantly. This means that a part of loosely bound polymer becomes tightly bound polymer, which does not participate in either of the two glass transitions. It is important to recognize that the transformation is gradual, as indicated by the variation of the area and $T_g$ of the second peak with the number of measurements performed on the sample. Annealing effects persist after the second run or after extensive heat treatment. In order for the gradual nature of the transformation and the decrease of the second $T_g$ to be explained, it is essential to realize that the chains in the loosely bound polymer cannot be described by a unique mobility; rather, they have to be described by a distribution of mobilities. The significant width of the second tan $\delta$ peak argues in favor of this assumption. Furthermore, it makes sense that the probability of the transformation taking place for a particular chain depends on the mobility of the chain. The lower the chain mobility, the higher is the probability that the chain will undergo the transformation to tightly bound during annealing. The higher the chain mobility, the lower is the probability of the transformation; hence, the first glass transition is not significantly affected by annealing. Moreover, the mobility distribution of the loosely bound polymer chains that arises after annealing is lacking the lowest mobility part of the original distribution, and thus its maximum is shifted to higher mobilities. In other words, the average mobility of the loosely bound polymer remaining after annealing is higher than that of the original loosely bound polymer before annealing, which in turn explains why the second $T_g$ decreases with annealing.

The reason for annealing effects being significant only for composites containing less than 20 wt % silica can be addressed by the proposed model. As discussed before, during annealing, part of the loosely bound polymer transforms to tightly bound polymer, through activated chain motions. At 20 wt % filler content, though, the regions of tightly bound polymer start to overlap, and any loosely bound polymer located in the space between the particles is transformed to tightly bound, since it experiences mobility restrictions from different particles. The result is that for composites containing more than 20 wt % silica, tightly bound polymer constitutes the main part of the polymeric material; hence, annealing effects are not significant for high particle contents.

## Conclusions

The interactions of polymer chains with very fine silica particles of high surface area restrict the mobility of the chains and lead to the formation of tightly bound and loosely bound polymer. The second tan $\delta$ peak in the mechanical measurements of several filled polymers is assigned to the glass transition of the loosely bound polymer. The notion that mobility restrictions lead to a new glass transition is thus established, supporting this aspect of the model of the morphology of random ionomers, proposed by Eisenberg, Hird, and Moore (EHM model). The detailed characteristics of the new glass transition were found to depend on the nature and the molecular weight of the polymer, as well as the filler content and the thermal history of the composite. These results were interpreted through a proposed schematic model. According to the model, the second glass transition appears only after overlap of the regions of loosely bound polymer is achieved, at *ca.* 10 wt % silica. As the filler content increases further, the average interparticle distance decreases and the mobility restrictions on the loosely bound polymer become so severe that it is progressively immobilized.

## References and Notes


(1) (a) Eisenberg, A.; King, M. *Ion-containing polymers*; Academic: New York, 1977. (b) Tant, M. R.; Wilkes, G. L. *J. Macromol. Sci., Rev. Macromol. Chem. Phys.* **1988**, *C28*, 1. (c) Mauritz, K. A. *J. Macromol. Sci., Rev. Macromol. Chem. Phys.* **1988**, *C28*, 65. (d) Fitzgerald, J. J.; Weiss, R. A. *J. Macromol. Sci., Rev. Macromol. Chem. Phys.* **1988**, *C28*, 99. (e) Latman, C. W.; MacKnight, W. J.; Ludberg, R. D. In *Comprehensive Polymer Science*; Allen, G., Bevington, J. C., Eds.; Pergamon: Oxford, U.K., 1989; Vol. 2, Chapter 25. (f) *Ionomers: Characterization, Theory, and Applications*; Schlick, S., Ed.; CRC: Boca Raton, FL, (in preparation). (g) Ionomers: *Synthesis, Structure, Properties, and Applications*; Tant, M. R., Mauritz, K. A., Wilkes, G. L., Eds.; Van Nostrand Reinhold, New York (in press). (h) Kim, J.-S.; Eisenberg, A. *Introduction to Ionomers*; Carl Hanser Verlag: München (in preparation).

(2) Eisenberg, A.; Hird, B.; Moore, R. B. *Macromolecules* **1990**, *23*, 4098.

(3) (a) MacKnight, W. J.; Taggart, W. P.; Stein, R. S. *J. Polym. Sci., Polym. Symp.* **1974**, *45*, 113. (b) Marx, C. L.; Caulfield, D. F.; Cooper, S. L. *Macromolecules* **1973**, *6*, 344.

(4) Yang, S.; Sun, K.; Risen, W. M., Jr. *J. Polym. Sci.; Polym. Phys. Ed.* **1990**, *28*, 1685.

(5) Yano, S.; Tadano, K.; Jérôme, R. *Macromolecules* **1991**, *24*, 6439.

(6) Gao, Z.; Zhong, X.-F.; Eisenberg, A. *Macromolecules* **1994**, *27*, 794.

(7) (a) Vanhoorne, P.; Jérôme, R.; Teyssié, P.; Lauprêtre, F. *Macromolecules* **1994**, *27*, 2789. (b) McBrierty, V. J.; Smyth, G.; Douglas, D. C. In *Structure and Properties of Ionomers*; Pineri, M., Eisenberg, A., Eds.; NATO ASI Series C, Vol. 198; Reidel: Dordrecht, 1986.

(8) Kim, J.-S.; Jackman, R. J.; Eisenberg, A. *Macromolecules* **1994**, *27*, 2789.

(9) (a) *Reinforcement of Elastomers*; Kraus, G., Ed.; Wiley: New York, 1965. (b) Donet, J. B.; Voet, A. *Carbon Black Physics, Chemistry and Elastomer Reinforcement*; Marcel Decker: New York, 1976. (c) *Filled Polymers I, Science and Technology*; Enikolopyan, N. S., Ed.; Advances in Polymer Science 96; Springer-Verlag: Berlin, 1990. (d) Kraus, G. In Advances in Polymer Science 8; Springer-Verlag: Berlin, 1971; p 155. (e) Blow, C. M. *Polymer* **1973**, *14*, 309. (f) Kraus, G. *Angew. Makromol. Chem.* **1977**, *60/61*, 215. (g) Medalia, A. I. *Rubber Chem. Technol.* **1978**, *51*, 437. (h) Boonstra, B. B. *Polymer* **1979**, *20*, 691. (i) Rigbi, Z. *Rubber Chem. Technol.* **1982**, *55*, 1181. (j) Dannenberg, E. M. *Rubber Chem. Technol.* **1986**, *59*, 512. (k) Nakajima, N.; Chu, M. H. *Rubber Chem. Technol.* **1990**, *63*, 110.

(10) Kraus, G.; Gruver, J. T. *J. Polym. Sci., Polym. Phys. Ed.* **1970**, *8*, 571.

(11) (a) Privalko, V. P.; Lipatov, Yu. S.; Kercha, Yu. Yu.; Mozshukhina, L. V. *Vysokomol. Soyedin.* **1971**, *A13*, 103. (b) Lipatov, Yu. S.; Privalko, V. P. *Vysokomol. Soyedin.* **1972**, *A14*, 1643.

(12) Higgins, J. S.; Arrighi, V.; Floudas, G. *ISIS Experimental Report*; 1993.

(13) Kaufman, S.; Slichter, W. P.; Davis, D. D. *J. Polym. Sci., Polym. Phys. Ed.* **1971**, *9*, 829.

(14) O'Brien, J.; Cashell, E.; Wardell, G. E.; McBrierty, V. J. *Macromolecules* **1976**, *9*, 653.

(15) Dutta, N. K.; Choudhury, N. R.; Haidar, B.; Vidal, A.; Donnet, J. B.; Delmotte, L.; Chezeau, J. M. *Polymer* **1994**, *35*, 4293.

(16) Ito, M.; Nakamura, T.; Tanaka, K. *J. Appl. Polym. Sci.* **1985**, *30*, 3493.

(17) Pliskin, I.; Tokita, N. *J. Appl. Polym. Sci.* **1972**, *16*, 473.

(18) Ecker, R. *Kautsch. Gummi Kunstst.* **1968**, *21*, 304.

(19) Yim, A.; Chahal, R. S.; St. Pierre, L. E. *J. Colloid Interface Sci.* **1973**, *43*, 583.

(20) Landry, C. J. T.; Coltrain, B. K.; Landry, M. R.; Fitzgerald, J. J.; Long, V. K. *Macromolecules* **1993**, *26*, 3702.

(21) Zheng, X.; Saver, B.; Van Alsten, J.; Rafailovich, M.; Sokolov, J.; Schwartz, S. A.; Rubinstein, M. To be published in *Phys. Rev. Lett.*

(22) (a) Van Alsten, J.; Granick, S. *Macromolecules* **1990**, *23*, 4856. (b) Hu, H. W.; Carson, G. A.; Granick, S. *Phys. Rev. Lett.* **1991**, *66*, 2758. (c) Granick, S. *Science* **1991**, *253*, 1374.

(23) Schüller, J.; Mel'nichenko, Yu. B.; Richert, R.; Fischer, E. W. *Phys. Rev. Lett.* **1994**, *73*, 2224.

(24) (a) Bitsanis, I.; Hadjioannou, G. *J. Chem. Phys.* **1990**, *92*, 3827. (b) Bitsanis, I.; Pan, C. *J. Chem. Phys.* **1993**, *99*, 5520.

(25) Tsagaropoulos, G.; Eisenberg, A. *Macromolecules* **1995**, *28*, 396.

(26) Smith, P.; Eisenberg, A. *Macromolecules* **1994**, *27*, 545.

(27) (a) *Chromatographic Theory and Basic Principles*; Jonsson, J. A., Ed.; Marcel Dekker: New York, 1987. (b) Rundel, R. *PeakFit™ v.3.0 Technical Guide*; Jandel Scientific: 1991.

(28) Kosmas, M. K. *Macromolecules* **1990**, *23*, 2061.

(29) (a) Deng, Z.; Schreiber, H. P. In *Contemporary Topics in Polymer Science*; Culbertson, B. M., Ed.; Plenum: New York, 1989; Vol. 6, pp 385–400. (b) Panzer, U.; Schreiber, H. P. *Macromolecules* **1992**, *25*, 3633. (c) Bosse, F.; Eisenberg, A.; Deng, Z.; Schreiber, H. P. *J. Adhesion Sci. Technol.* **1993**, *7*, 1139. (d) Bosse, F.; Eisenberg, A.; Xu, R.; Schreiber, H. P. *J. Appl. Polym. Sci.* **1994**, *51*, 521.

(30) Vilgis, T. A.; Heinrich, G. *Macromolecules* **1994**, *27*, 7846.

(31) (a) Rochow, E. G.; LeClair, H. G. *J. Inorg. Nucl. Chem.* **1955**, *1*, 92. (b) Rochow, E. G. *Silicon and Silicones*; Springer-Verlag: Berlin, 1987.

(32) Tsagaropoulos, G. Ph.D. Thesis, Brown University, 1993.

(33) Kraus, G.; Rollmann, K. W.; Gruver, J. T. *Macromolecules* **1970**, *3*, 92.

(34) Lipatov, Yu. S.; Moisya, Ye. G.; Semenovich, G. M. *Vysokomol. Soyedin.* **1977**, *A19*, 125.


MA950288Q